Optical manipulation and study of single gold nanoparticles in solution

Ruijgrok, P.V.

5

Measuring the temperature of a single metal nanoparticle by changes of the plasmon spectral width

In this chapter we present preliminary results on the temperature dependence of the spectral width of the plasmon resonance of a single gold nanoparticle, and its use to measure the temperature of the particle.

5.1 Introduction

In a wide variety of experiments, it is interesting to locally measure temperatures with a local temperature probe.[139–141] The range of operation temperatures, the accuracy of the temperature determination, and the temporal and spatial resolution determine the range of application for each given temperature probe. The use of nano-objects as thermometers is promising due to their small size and short thermal relaxation times, enabling both high spatial and temporal resolution.

In optical experiments on metal nanoparticles it is often required to estimate the temperature of a particle that is heated by absorption of the illumi-

nation light. Commonly, the temperature increase of an illuminated nanoparticle is estimated from a calculation of the power absorbed by the particle and the dissipation of heat into the particle environment, as given by Fourier's law of heat conduction. However, in practical experiments at least one of the required parameters –the absorption cross-section of the particle, the local illumination intensity, the particle radius or the thermal conductivity– is often not accurately known, resulting in large uncertainties in the temperature estimation.

To obtain more reliable estimates of particle temperature, various methods have been developed that measure the particle temperature indirectly, by characterization of some physical property of the environment of the particle. Examples come from optical trapping, where a particle temperature can be inferred from the scaling of the amplitude of Brownian fluctuations with trapping power,[77,142] as presented also in Chapter 4. Recently, an elegant approach was presented by Bendix *et al.*,[88] who used the known temperature of a melting transition in a lipid bilayer to probe the temperature profile around a trapped particle. The hot region of the membrane close to the particle could be identified by fluorophores that favored one of the membrane phases. Baffou *et al.*[140] have used the polarization anisotropy of fluorescent dye molecules to probe the temperature around metal nanostructures. However, the need for an optical trap, a lipid membrane or fluorescent dyes limits the range of applications of these approaches. To have a temperature sensor that can be used in the same way in a variety of experimental configurations, a temperature-dependent optical effect of the particle itself is desirable.

Here, we set out to explore the possibility to measure the temperature of single gold nanoparticles from temperature-induced changes of the width of their plasmon resonance. The idea is that the temperature dependence of the damping of a plasmon excitation is known accurately. When contributions from interband transitions can be neglected, as is the case for gold nanorods with a longitudinal plasmon resonance below $\approx$ 2eV, the temperature dependence of the plasmon relaxation γ rate is determined by the temperature dependence of electron-phonon decay rate in the metal. Around room temperature (well above the Debye temperature of the metal), the decay rate increases linearly with temperature, a convenient feature for a thermometer. The plasmon relaxation rate $\gamma(\omega)$ at a frequency ω is observed experimentally as the spectral linewidth $\Gamma(\omega)$ of the plasmon resonance. Scattering spectra of individual gold nanoparticles can be readily measured with relatively simple equipment. As the only experimental restriction is that a scattering spectrum can be measured, the method would be applicable to variety of experimental

configurations.

In this chapter, we present two novel single-particle approaches to test wether the changes of the spectral width can serve as a single-particle thermometer. First we calibrate the method on immobilized gold nanorods in a temperature-controlled sample chamber, where temperature is varied in a range 290 K-340 K. Secondly, we apply the method to optically trapped gold nanorods, an example of an experimental system where temperature is an important parameter that is difficult to estimate.

5.2 Experimental

The experimental setups used for the two approaches to study the temperature dependent plasmon damping are shown in Fig. 5.1.

Experiments on immobilized particles are performed with a metal sample holder that can be brought to a controlled temperature by means of circulating water heated by a laboratory temperature controller, Fig. 5.1 (a-b). The temperature of the metal chamber is measured by a temperature sensor (platinum resistor) inserted in the center of the chamber. Two coverslips separated by immersion oil are clamped to the sample holder with a metal ring that is in good thermal contact with the chamber, to assure a constant temperature over the region between the temperature sensor and the gold nanoparticles. The metal sample holder is mounted on a piezo-scanner to enable three-dimensional positioning with nanometer accuracy. The chamber is thermally isolated from the scanner to minimize thermal drifts and prevent scanner damage. In the experiment single particles are followed over a temperature range of 50 K. Over this range, the residual thermal drift in the microscope is still several tens of microns, large enough for the nanoparticles under study to completely drift out of the microscope's field of view. To follow single particles over the complete temperature range, the temperature of the sample chamber was changed in small steps ($\approx$ 2 K) and thermal drifts were compensated by manually adjusting the piezo-scanner to keep the particle in focus.

The optical trap setup show in Fig. 5.1 (c-d) is as previously described in Chapter 3. Briefly, an infrared cw beam (wavelength 1064 nm) is focused by a NA = 1.4 oil immersion objective, about 25 μm into water in a home built flow cell.

Gold nanorods were synthesized by silver-assisted seed-mediated growth in the presence of hexadecyltrimethylammonium bromide (CTAB).[119] The

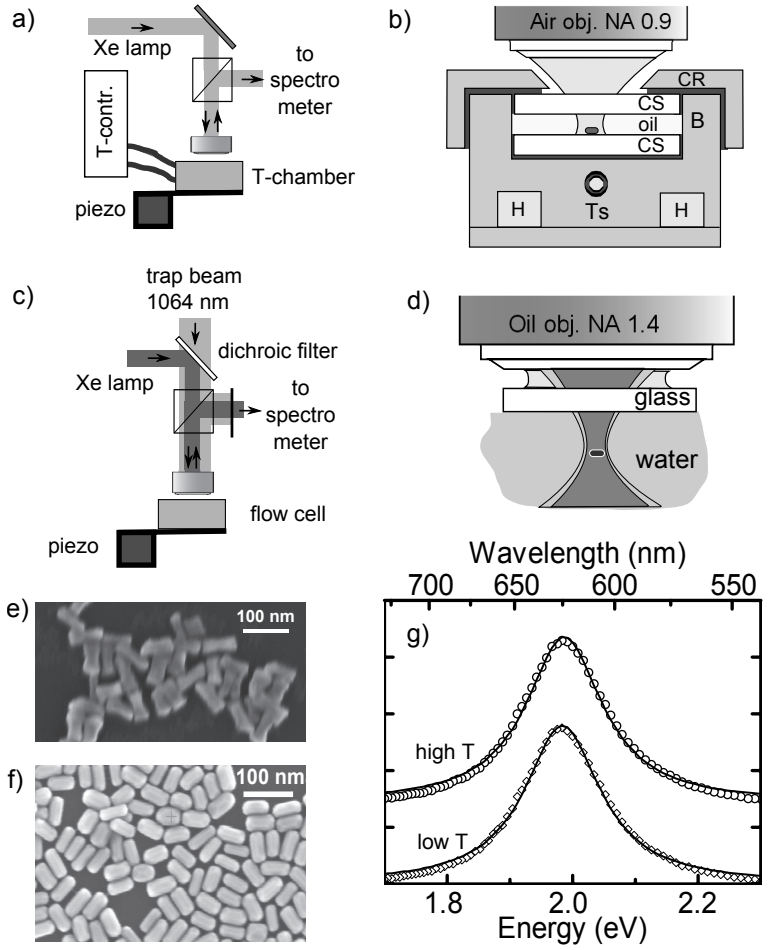

Figure 5.1: Schematic overview of the two experimental approaches to study the temperature dependence of plasmon damping. a) Schematic of the setup to record white light scattering spectra of single gold nanoparticles immobilized on a glass substrate, in a temperature controlled chamber. b) Detail of the chamber. CS, coverslip; B, metal heater block; CR, metal clamp; H, heater channel with water flow from T-controller; Ts, temperature sensor. c) Schematic of the optical trapping setup. d) Detail of the trap focus in the flow cell. e) Gold nanorods (33 nm width, 74 nm length) used for the experiments on immobilized particles. f) Gold nanorods (25 nm width, 60 nm length) used in the optical trapping experiments. d) Typical scattering spectra of an optically trapped gold nanorod, showing the longitudinal plasmon resonance. The two spectra were taken at the maximum (high T, open circles) and minimum (low T, open diamonds) trap power, and are offset for clarity. The spectra are very similar, but the Lorentzian fits (solid lines) resolve a small broadening and blue-shift of the high temperature spectrum, with respect to the low temperature spectrum.

experiment with immobilized particles was performed with gold nanorods (33 nm mean diameter by 74 nm mean length) that were coated with (3-Mercaptopropyl)trimethoxysilane (MPTS, Sigma-Aldrich) following Liz-Marzán *et al.*[143] to increase the thermal stability of the nanorod. A sample with single well-separated rods was obtained by spin-coating on a microscope coverslip. The experiments in the optical trap were performed with gold nanorods of 25 nm mean diameter and 60 nm width. These nanorods were coated with thiolated polyethyleneglycol (PEG, M_W = 5kDa, Sigma Aldrich) coated to prevent their aggregation in pure water.[120] The rod suspensions were diluted by several orders of magnitude to prevent the trapping of multiple particles during a measurement. White light scattering spectra were measured as previously described in Chapter 3: the rods were excited with unpolarized light from a Xe-lamp, and backscattered light from the rods was detected through a pinhole. For immobilized particles, no polarizer was placed in the detection path.

5.3 Modeling of plasmon damping

We briefly review the mechanisms responsible for damping of a plasmon excitation in a gold nanoparticle, with a focus on their temperature dependence. A more in-depth treatment has been given by, for example, Liu *et al.*[123]

The total damping rate γ of a plasmon excitation in a metal nanoparticle is determined by damping rate γ_b due to mechanisms present in the bulk metal plus a rate γ_np due to damping mechanisms present in nanoparticles only, via

$$\gamma = \gamma_\mathrm{b} + \gamma_\mathrm{np} \tag{5.1}$$

In the bulk metal, the plasmon relaxation rate is the sum of a decay rate γ_{e-e} due to electron-electron scattering and the electron-phonon scattering rate γ_{e-p}:

$$\gamma_\mathrm{b} = \gamma_{e-e} + \gamma_{e-p}(T). \tag{5.2}$$

Of the two mechanisms, only γ_{e-p} depends significantly on temperature.[123] The electron-phonon scattering is calculated by considering a free electron gas and a Debye model for phonons. In the absence of interband transitions the damping rate is given by[123]

$$\gamma_{e-p}(T) = \hbar\tau_0^{-1}\left[\frac{2}{5} + 4\left(\frac{T}{\Theta}\right)^5 \int_0^{\Theta/T} \frac{z^4}{e^z - 1} dz\right] \tag{5.3}$$

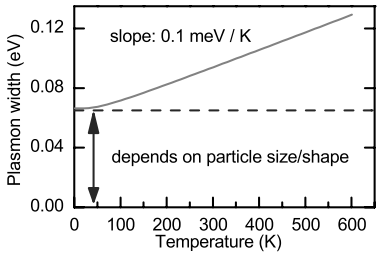

Figure 5.2: Calculated plasmon damping as a function of temperature, following the model of Liu et al.[123] In the absence of interband transitions, the temperature dependence is determined by the temperature dependence of electron-phonon coupling only. At room temperature and above, it varies linearly with temperature.

where τ_0 is a material-dependent constant, and Θ is the Debye temperature. Eq. 5.3 is derived in the limit $E_F >> \hbar\omega >> k_B T$ and $k_B\Theta$, with E_F the Fermi energy. These requirements are satisfied for gold at plasmon energies around 2 eV. For gold, $\tau_0 = 30$ fs and $\Theta = 185$ K.[144]

The bulk damping rate γ_B evaluated with Eq. 5.3 for gold, and the expression for γ_{e-e} taken from Liu *et al.*[123] is shown in Fig. 5.2. At room temperature and above, the damping increases almost linearly with temperature, with a slope 0.1 meV/K.

In nanoparticles, radiation of the plasmon forms an extra damping mechanism with a rate γ_r, independent of temperature at optical frequencies.[123] In addition, the bulk electron scattering rate has to be modified to take into account electron surface scattering, contributing a rate γ_S, also temperature independent. Both radiative damping and electron surface scattering depend on the particle radius R, varying as R^3 and $1/R$ respectively. The plasmon width thus varies with particle size. However, within the limits of our model the temperature dependence of the plasmon width results only from the temperature dependence of the electron-phonon scattering rate, which is independent of particle size. The temperature-induced change of the plasmon width, which increases linearly with temperature with a known proportionality constant, can serve as a thermometer.

Experiments on ensembles of immobilized gold bipyramids[123] have confirmed the dominant role of electron-phonon scattering in the temperature dependence of the damping of the plasmon resonance of the nanoparticles, and were in quantitative agreement with the above model. A question remains how accurately the parameter τ_0 describes different samples or different individual particles within a sample. The parameter τ_0 is normally

obtained from the infrared absorption of bulk metals. As reviewed by Winsemius,[145] the infrared absorbtion of metals has been shown to vary with crystal structure, concentration of defects or impurities and surface roughness.[146–149]

We emphasize that the above modeling holds only in the absence of interband transitions. When the contribution of interband transitions cannot be neglected, the modeling needs to be re-evaluated. Although the modeling may be more involved than for the case of intraband transitions, the temperature dependence of interband transitions is known,[150] and may thus also serve as a thermometer. Such an analysis may be then be used to evaluate the temperature dependence of plasmon damping in spherical gold nanoparticles. For these particles, the contribution of interband transitions can not be neglected, as the plasmon resonance occurs around 2.4 eV, in the region of interband transitions. For the longitudinal plasmon resonance of the gold nanorods used in this Chapter, with resonance energy < 2 eV, the contribution of interband transitions is still small, so that the above modeling applies.

5.4 Results and discussion

5.4.1 Temperature dependence of the plasmon width of immobilized gold nanorods

Figure 5.3 displays the results obtained on immobilized single gold nanorods in a temperature- controlled sample chamber. Scattering spectra as in Fig. 5.1 (g) were recorded for a number of single gold nanorods at a given temperature. A series of such measurements were made from room temperature upwards to 340 K and then downwards back to room temperature. Panel a) and b) show a typical spectral width (full width at half maximum, FWHM) and resonance energy observed in a measurement series on a single gold nanorod, obtained from Lorentzian fits of the measured scattering spectra .

A broadening of the plasmon resonance as a function of temperature is clearly observed in Fig. 5.3 a). Note that the change of the plasmon width is not large compared to the plasmon width itself; over the full temperature range the plasmon width changes by less than 3 percent. However, changes of this magnitude are easily resolved from the fits of the scattering spectra, due to the high signal-to-noise. A small anomaly to the overall trend is seen in the first three acquired data points –at the lowest temperatures of the upwards series– displaying a plasmon narrowing with increasing temperature. This effect is not reproduced in the downward measurement series that was

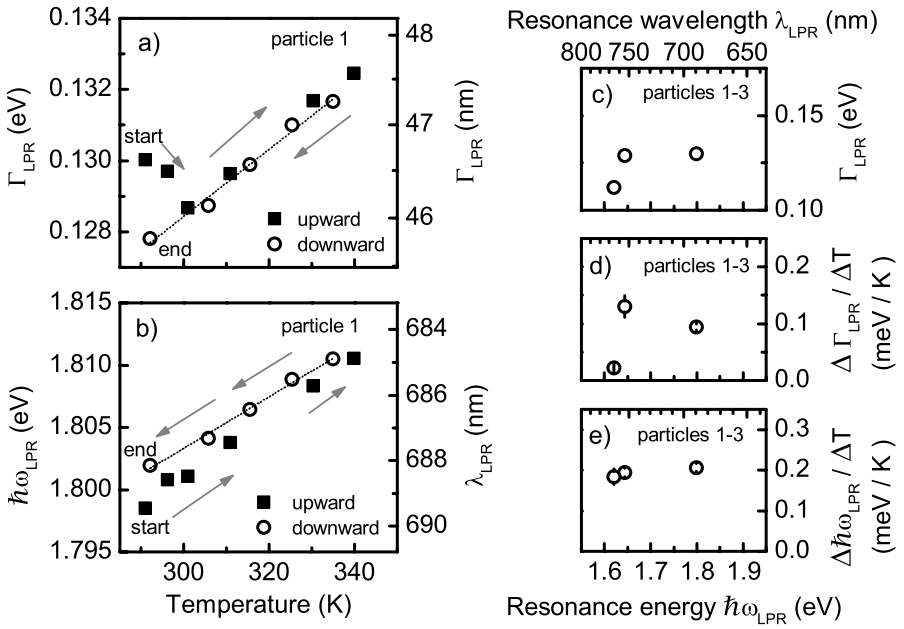

Figure 5.3: Temperature dependence of the longitudinal plasmon resonance of single gold nanorods, immobilized on a glass substrate and surrounded by immersion oil. (a) Width Γ_{LPR} and (b) energy $\hbar\omega_{LPR}$ of the longitudinal plasmon resonance of an individual gold nanorod. Data was taken first going upwards in temperature, then downwards back to room temperature at 290 K. The dotted lines are linear fits of the data from the series downwards in temperature. (c-e) Measured temperature dependence of the plasmon for the nanorod in (a-b), plus two additional rods, as a function of the longitudinal plasmon resonance energy $\hbar\omega_{LPR}$ of the rods. Panel c): Width Γ_{LPR}(at 290 K) of the rods. Panels (d) and (e) display respectively the temperature dependence of the plasmon width and energy, obtained from the slopes of the linear fits as in (a-b).

acquired subsequently, indicating that an irreversible change to the particle may have occurred. An explanation of this change could be the removal of part of the MPTS capping layer of the rod, diminishing the effect of chemical interface damping on the particle. Independently of the origin of such irreversible changes, over the complete series a temperature-induced broadening is robustly observed: the linear temperature dependence of the plasmon width is identical in both upward and downward measurement series, within experimental error. The measured temperature-induced broadening is 0.1 ± 0.01 meV/K. This value is good agreement with the value of 0.1 meV/K

that is expected in the absence of inter-band transitions, due to the increase of electron-phonon scattering rate with temperature.

Similar results were obtained on two other single gold nanorods, as summarized in Fig. 5.3 (c-e). On all three nanorods a temperature-induced broadening is observed, see Fig. 5.3 d). However, while for two of the gold nanorods the temperature-induced broadening is around the expected value of 0.1 meV/K, on one of the rods the broadening is much smaller. The reason for this deviation is currently not understood.

The experiment on immobilized particle shows that the temperature-induced broadening of the plasmon resonance can be measured on a single gold nanoparticle. The experimentally measured broadening is close to the value expected if the temperature dependence of plasmon damping is determined by electron-phonon scattering only. However, the quality of our experiment is as yet good not enough to serve as an accurate calibration of our proposed method as single particle thermometer. We expect to be able to improve the quality of our calibration experiment by performing measurements on more individual particles. To test the validity of the method more thoroughly, experiments should be repeated for rods with a broader range of aspect ratios, thus probing a range of plasmon energies. Additionally, it will be instructive to perform measurements on gold spheres, to quantify the influence of interband transitions on the temperature dependence of plasmon damping.

We end our discussion by observing that all three investigated particles display a temperature-induced blue-shift of the plasmon energy, see Fig. 5.3 e). As the effect is accurately observed –the detected blue-shift is within experimental error the same on all particles– it may seem an attractive alternative to exploit as thermometer. However, we believe that the temperature dependence of the plasmon energy is not suitable as a thermometer, because the shift may vary for different experimental conditions, and is difficult to model. The reason is that several effects of different physical origins shift the plasmon as a function of temperature. Thermal expansion causes a red-shift of the plasmon, due to a lowered electron density. Most dielectric media display a lowering of the refractive index with increasing temperature, causing a blue-shift of the plasmon. The temperature dependence of the refractive index of the medium surrounding the particles is not always known.

5.4.2 Temperature dependence of the plasmon width of optically trapped gold nanorods

The optical trapping of gold nanoparticles is an example of a class of experiments where the particle temperature is an important parameter that is difficult to estimate accurately.

Before discussing our experimental results on optically trapped particles, it is instructive to consider how the difficulty in the temperature estimation arises. Although some of the encountered difficulties are specific to optical trapping only, similar issues are met frequently in optical microscopy experiments on metal nanoparticles.

Heating of the particles in the optical trap is induced by absorption of the trap laser. The temperature increase ΔT of a trapped nanorod is given by Fourier's law of heat conduction. Specifically, for the case of a spherical particle with a thermal conductivity much higher than that of the environment, the temperature is given in steady-state by the expression

$$\Delta T = \frac{I\sigma_{\text{abs}}}{4\pi R K_m}, \tag{5.4}$$

where σ_{abs} is the absorption cross-section at the trap wavelength, I is the local intensity of the trap laser, R is the radius of the sphere and K_m is the thermal conductivity of the medium. The heat dissipation of nanorods of moderate aspect ratio (smaller than 5) can be well approximated by the heat dissipation of a sphere with the volume of the rod, see Appendix G.

In optical trapping experiments, single nanoparticles are selected at random from a given sample. The inevitable distribution of particle sizes and shapes in the ensemble results in a distribution of absorption cross-sections σ_{abs} and radii R of the trapped particles, leading to uncertainty in the evaluation of Eq. 5.4.

An additional complication arises because the local intensity of the trap is difficult to determine accurately in the experiment. The local intensity is normally obtained from calculation, by assuming a diffraction limited focal spot for a certain numerical aperture. However, the wavelengths typically used in optical trapping are in the near-infrared, far from the visible region for which most commercial high-numerical-aperture objective are designed. The aberrations that result can enlarge the focal spot and significantly lower the local intensity. In addition, in some cases spherical aberrations are introduced due to the refractive index mismatch of coverslips and the liquid medium, as encountered in Chapters 3 and 4. These aberrations can be compensated in various ways[118,151] and/or quantified experimentally, but obtaining an accurate

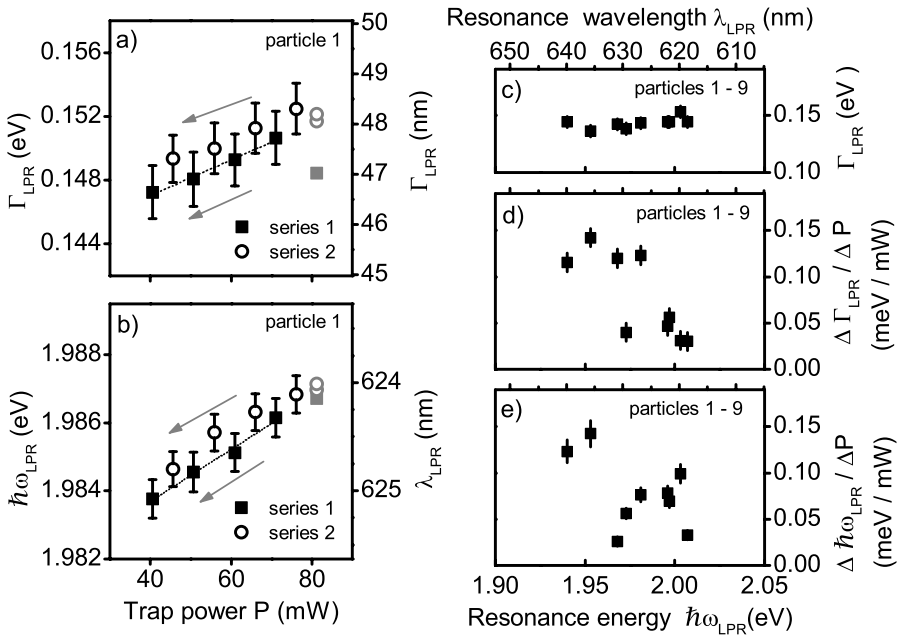

Figure 5.4: Temperature dependence of the plasmon resonance of single optically trapped gold nanorods in water, via laser-induced heating of the rods. A typical result obtained on a single trapped nanorod is shown in panels (a) and (b), displaying the width and energy of the rod as functions of trapping power. Black solid squares and black open circles are two consecutive measurement series on the same nanorod, taken going downward in trapping power. Grey solid squares and gray open circles indicate the plasmon width and energy before the start of the corresponding measurement series. Dotted lines are linear fits to the first series 1 with slopes $(1.0 \pm 0.09) \cdot 10^{-4}$ eV/ mW (a) and $(0.8 \pm 0.1) \cdot 10^{-4}$ eV/mW (b), respectively. (c-e) Temperature dependence the plasmon resonance obtained from linear fits to the data as presented in panel (a-b), for 9 single trapped gold nanorods. The data are plotted as functions of the rods' longitudinal plasmon resonance energy. Panel (c): Width of plasmon resonance of the rods at zero trap power. Panels (d) and (e) display respectively the variation of plasmon width and energy with trapping power.

determination of the absolute value of the local intensity remains challenging.

In Fig. 5.4 we examine the temperature dependence of the plasmon resonance of single gold nanorods in an optical trap. Here, the temperature of the rods is controlled indirectly by variation of the trapping power. Figures 5.4 (a) and (b) show a typical result obtained on a single gold nanorod in the op-

tical trap. As expected, we observe a broadening of the longitudinal plasmon resonance of the particle as the trapping power is increased, see Fig. 5.4 (a). The figure displays two series of measurements on the same gold nanorod. The data points in each series were taken within about 2 minutes, whereas the two series were separated in time by about 10 min. In the second series a small overall broadening of the plasmon is seen. The reason for this increased plasmon damping is not clear. Significant reshaping is excluded, as the longitudinal plasmon resonance remains at its initial value to within 0.1%. The small additional damping may be related to thermally induced changes of the structure of the particle, for example an increased surface roughness. The slope of the lines is $1.0 \pm 0.1 \cdot 10^{-4}\,\mathrm{eV/mW}$. According to the calculation in section 5.3, this corresponds to a temperature increase of $1\,\mathrm{K/mW}$. This is close to the value of $0.9\,\mathrm{K/mW}$ found for this particular rod in the measurements of Brownian fluctuations presented in Chapter 4.

We measured a number of individual gold nanorods in the trap. As seen in Fig. 5.4 (c-d), all particles qualitatively displayed the same behavior as observed for the rod in Fig. 5.4 (a-b). On average, the rods with a longer longitudinal plasmon resonance wavelength (larger aspect ratio) display a larger increase of the plasmon width as function of trapping power. This is expected, as the resonance wavelength of these rods is closer to the trap wavelength, resulting in larger absorption cross-sections and higher temperatures. The spread of values in Fig. 5.4 d) indicates that different particle temperatures occur at a given trap power and rod aspect ratio (or resonance wavelength). This spread is most likely due to the spread in volumes of the particles in the sample.

We end our discussion by noting that in the analysis of the scaling of trap parameters as a function of trap power in Chapter 4, we have assumed a linear dependence of the temperature increase with trapping power. With a thermally induced broadening of the particle's plasmon resonance, this assumption no longer strictly holds. However, we note that the temperature-induced broadening is small, resulting in a plasmon broadening of less than 5 percent between zero and maximum trap power. A broadening of this magnitude is not expected to qualitatively change any of the previously obtained results, although some of the obtained values may be altered in a minor way.

5.5 Conclusions

We have presented an experimental study of the temperature dependence of the plasmon resonance in single gold nanoparticles, motivated by the possible use of temperature-induced broadening of the plasmon as a thermometer. We have investigated immobilized single gold nanorods in a calibrated temperature chamber, and gold nanorods in an optical trap. In all experiments, a broadening of the plasmon is observed when temperature is increased, and the amount of broadening is close to the expected value. However, a distribution of responses is observed for different single immobilized nanorods for the same temperature increments. As this behavior is not yet understood, the validity of the proposed method as thermometer remains to be proven.